Title

Calix[4]arene-linked bisporphyrin hosts for fullerenes: binding strength, solvation effects, and porphyrin-fullerene charge transfer bands.

Permalink

https://escholarship.org/uc/item/9345z3m5

Journal

Journal of the American Chemical Society, 128(49)

ISSN

0002-7863

Authors

Hosseini, Ali
Taylor, Steven
Accorsi, Gianluca
et al.

Publication Date

2006-12-01

DOI

10.1021/ja066031x

Peer reviewed

Calix[4]arene-Linked Bisporphyrin Hosts for Fullerenes: Binding Strength, Solvation Effects, and Porphyrin−Fullerene Charge Transfer Bands

Ali Hosseini,[†] Steven Taylor,[†] Gianluca Accorsi,[‡] Nicola Armaroli,*[,‡]
Christopher A. Reed,*[,§] and Peter D. W. Boyd*[,†]

*Contribution from the Department of Chemistry, The University of Auckland,
Private Bag 92019, Auckland, New Zealand, Molecular Photoscience Group, Istituto per la
Sintesi Organica e la Fotoreattività (ISOF), Consiglio Nazionale delle Ricerche (CNR),
Via Gobetti 101, 40129 Bologna, Italy, and Department of Chemistry, University of California,
Riverside, California 92521*

Received August 18, 2006; E-mail: chris.reed@ucr.edu; pdw.boyd@auckland.ac.nz; armaroli@isof.cnr.it

Abstract: A calix[4]arene scaffolding has been used to construct bisporphyrin ("jaws" porphyrin) hosts for supramolecular binding of fullerene guests. Fullerene affinities were optimized by varying the nature of the covalent linkage of the porphyrins to the calixarenes. Binding constants for C_{60} and C_{70} in toluene were explored as a function of substituents at the periphery of the porphyrin, and 3,5-di-*tert*-butylphenyl groups gave rise to the highest fullerene affinities (26 000 M^{-1} for C_{60}). The origin of this high fullerene affinity has been traced to differential solvation effects rather than to electronic effects. Studies of binding constants as a function of solvent (toluene < benzonitrile < dichloromethane ≪ cyclohexane) correlate inversely with fullerene solubility, indicating that desolvation of the fullerene is a major factor determining the magnitude of binding constants. The energetics of fullerene binding have been determined in terms of ΔH and ΔS and are consistent with an enthalpy-driven, solvation-dependent process. A direct relationship between supramolecular binding of a fullerene guest to a bisporphyrin host and the appearance of a broad NIR absorption band have been established. The energy of this band moves in a predictable manner as a function of the electronic structure of the porphyrin, thereby establishing its origin in porphyrin-to-fullerene charge transfer.

Introduction

Fullerenes and porphyrins possess unique redox and photo-electronic properties that make them highly suitable chromophores for the assembly of photoactive fullerene−porphyrin constructs. With irradiation, these assemblies can undergo photoinduced electron transfer (PET) between the donor porphyrin and the acceptor fullerene. Early studies of covalently linked fullerene−porphyrin dyads showed PET from the first excited singlet state of the porphyrin to the fullerene, with a high quantum yield.[1,2] Extensive work since then has shown that the small three-dimensional reorganization energies of fullerenes, following rapid electron transfer, slow the back electron transfer rate.[3−8] This helps move the charge recombina-

tion reaction into the Marcus inverted region, as in the photosynthetic reaction center (PRC). The PRC achieves long-lived charge separation using a sequence of short-range electron transfer reactions along a redox gradient, leading to a spatially and electronically separated radical ion pair consisting of a bacteriochlorophyll dimer radical cation (the "special pair") and a quinone radical anion. Recently, using elaborate combinations of covalently connected porphyrin donors and fullerene acceptors, along with auxiliary ferrocene acceptors, the key features of this process have been duplicated with lifetimes comparable to the PRC.[9−11]

Covalent methods of linking fullerenes and porphyrins have been augmented by coordinate,[12−15] supramolecular,[16−24] and

† Auckland University.

‡ CNR-ISOF.

§ University of California, Riverside.

(1) Liddell, P. A.; Sumida, J. P.; MacPherson, A. N.; Noss, L.; Seely, G. R.; Clark, K. N.; Moore, A. L.; Moore, T. A.; Gust, D. *Photochem. Photobiol.* **1994**, *60*, 537−541.

(2) Kuciauskas, D.; Lin, S.; Seely, G. R.; Moore, A. L.; Moore, T. A.; Gust, D.; Drovetskaya, T.; Reed, C. A.; Boyd, P. D. W. *J. Phys. Chem.* **1996**, *100*, 15926−15932.

(3) Guldi, D. M. Fullerenes. *Chem. Commun.* **2000**, 321−327.

(4) Guldi, D. M. *Chem. Soc. Rev.* **2002**, *31*, 22−36.

(5) Guldi, D. M. *Pure Appl. Chem.* **2003**, *75*, 1069−1075.

(6) Guldi, D. M.; Da Ros, T.; Braiuca, P.; Prato, M. *Photochem. Photobiol. Sci.* **2003**, *2*, 1067−1073.

(7) Imahori, H. *Org. Biomol. Chem.* **2004**, *2*, 1425−1433.

(8) Kobori, Y.; Yamauchi, S.; Akiyama, K.; Tero-Kubota, S.; Imahori, H.; Fukuzumi, S.; Norris, J. R., Jr. *Proc. Natl. Acad. Sci. U.S.A.* **2005**, *102*, 10017−10022.

(9) Guldi, D. M.; Imahori, H.; Tamaki, K.; Kashiwagi, Y.; Yamada, H.; Sakata, Y.; Fukuzumi, S. *J. Phys. Chem. A* **2004**, *108*, 541−548.

(10) Imahori, H.; Sekiguchi, Y.; Kashiwagi, Y.; Sato, T.; Araki, Y.; Ito, O.; Yamada, H.; Fukuzumi, S. *Chem.−Eur. J.* **2004**, *10*, 3184−3196.

(11) Gust, D.; Moore, T. A.; Moore, A. L. *Acc. Chem. Res.* **2001**, *34*, 40−48.

(12) Da Ros, T.; Prato, M.; Guldi, D.; Alessio, E.; Ruzzi, M.; Pasimeni, L. *Chem. Commun.* **1999**, 635−636.

(13) Armaroli, N.; Diederich, F.; Echegoyen, L.; Habicher, T.; Flamigni, L.; Marconi, G.; Nierengarten, J. F. *New J. Chem.* **1999**, *23*, 77−83.

(14) Trabolsi, A.; Elhabiri, M.; Urbani, M.; Delgado de la Cruz, J. L.; Ajamaa, F.; Solladie, N.; Albrecht-Gary, A.-M.; Nierengarten, J.-F. *Chem. Commun.* **2005**, 5736−5738.

(15) D'Souza, F.; Ito, O. *Coord. Chem. Rev.* **2005**, *249*, 1410−1422.

H-bonding methodologies.[25−27] We have chosen the supramolecular assembly route because of its versatility and simplicity. Fullerenes and porphyrins are naturally attracted to each other, and this new supramolecular recognition element allows the easy construction of host−guest complexes and novel 3D assemblies.[28]

The attraction of a fullerene to a porphyrin was first recognized in the molecular packing of a crystal structure of an early fullerene−porphyrin dyad.[29] Since then, the close approach (ca. 2.7 Å) of the fullerene to the center of the porphyrin has been found in dozens of the porphyrin−fullerene cocrystallates,[28] and the interaction persists in solution.

In order to obtain high binding constants in discrete host−guest complexes, two appropriately oriented porphyrins are necessary to complex the fullerene. Cyclic bisporphyrins, first designed by Aida, Tashiro, and co-workers, showed large binding constants and selectivities.[16,17] Acyclic porphyrin hosts were first prepared using Pd-linked 4-pyridylporphyrins,[18,19] and a variety of other scaffolds and linkers have been reported.[20−22,30,31] In the present work, we use a calixarene scaffold to hold two porphyrins at the required ca. 12 Å separation. Calixarenes have a very well developed derivatization chemistry on both the "upper" and "lower" rims,[32] allowing easy synthesis of bisporphyrin hosts. Two such systems have been reported and their fullerene binding capacities explored.[31,33]

Our approach has been to concentrate on lower-rim-appended bisporphyrins which allow systematic variation in the nature of the linkage (−X− in Figure 1), the type of porphyrin, its solubility properties, and, most importantly, lead to an understanding of the factors affecting fullerene binding constants.

Large fullerene binding constants are necessary for meaningful photophysical studies because such measurements must be done at low concentrations (i.e., low optical densities), where undesired dissociation becomes favored. Binding constants have
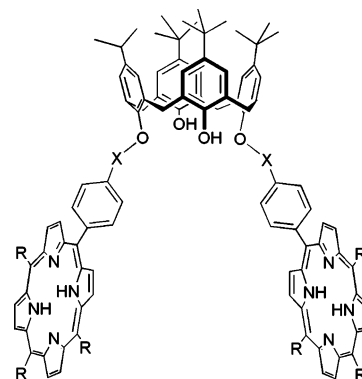

Figure 1. Schematic representation of a lower rim calixarene bisporphyrin with varied X linkers.

been reported for a variety of bisporphyrin hosts, but there is limited understanding of interplay of solvation energies, structural constraints, and electronic influences.[17,19] Another property in need of deeper understanding is the porphyrin-to-fullerene charge transfer absorption. Broad, low-energy absorptions (above 700 nm) have been reported in solid-state fullerene−porphyrin assemblies,[34−39] covalent dyads which allow the close approach of the chromophores,[40−48] and a supramolecular complex.[49] We will show in this paper that there is a direct relationship between supramolecular binding of the fullerene and the appearance of a NIR band. Moreover, the energy of this band can be systematically varied with porphyrin-type in an understandable manner. This band is important as a direct indicator of the energetics of the charge-separated state and, in combination with emission spectroscopy, leads to information on the lifetime of charge separation.

Results and Discussion

Synthesis and Structure. The six bisporphyrin calixarenes used in the present work are illustrated in Figure 2. All exploit trans-functionalization on the lower rim. Compound **1** has a

(16) Tashiro, K.; Aida, T.; Zheng, J.-Y.; Kinbara, K.; Saigo, K.; Sakamoto, S.; Yamaguchi, K. A. *J. Am. Chem. Soc.* **1999**, *121*, 9477−9478.
(17) Zheng, J.-Y.; Tashiro, K.; Hirabayashi, Y.; Kinbara, K.; Saigo, K.; Aida, T.; Sakamoto, S.; Yamaguchi, K. *Angew. Chem., Int. Ed.* **2001**, *40*, 1857−1861.
(18) Sun, D.; Tham, F. S.; Reed, C. A.; Chaker, L.; Burgess, M.; Boyd, P. D. W. *J. Am. Chem. Soc.* **2000**, *122*, 10704−10705.
(19) Sun, D.; Tham, F. S.; Reed, C. A.; Chaker, L.; Boyd, P. D. W. *J. Am. Chem. Soc.* **2002**, *124*, 6604−6612.
(20) Ayabe, M.; Ikeda, A.; Kubo, Y.; Takeuchi, M.; Shinkai, S. *Angew. Chem., Int. Ed.* **2002**, *41*, 2790−2792.
(21) Ayabe, M.; Ikeda, A.; Shinkai, S.; Sakamoto, S.; Yamaguchi, K. *Chem. Commun.* **2002**, *10*, 1032−1033.
(22) Wu, Z.-Q.; Shao, X.-B.; Li, C.; Hou, J.-L.; Wang, K.; Jiang, X.-K.; Li, Z.-T. *J. Am. Chem. Soc.* **2005**, *127*, 17460−17468.
(23) Kieran, A. L.; Pascu, S. I.; Jarrosson, T.; Sanders, J. K. M. *Chem. Commun.* **2005**, 1276−1278.
(24) Guldi, D. M.; Da Ros, T.; Braiuca, P.; Prato, M.; Alessio, E. *J. Mater. Chem.* **2002**, *12*, 2001−2008.
(25) Solladie, N.; Walther, M. E.; Gross, M.; Figueira Duarte, T. M.; Bourgogne, C.; Nierengarten, J.-F. *Chem. Commun.* **2003**, 2412−2413.
(26) D'Souza, F.; Chitta, R.; Gadde, S.; McCarty, A. L.; Karr, P. A.; Zandler, M. E.; Sandanayaka, A. S. D.; Araki, Y.; Ito, O. *J. Phys. Chem. B* **2006**, *110*, 5905−5913.
(27) Solladie, N.; Walther, M. E.; Herschbach, H.; Leize, E.; Van Dorsselaer, A.; Figueira Duarte, T. M.; Nierengarten, J.-F. *Tetrahedron* **2006**, *62*, 1979−1987.
(28) Boyd, P. D. W.; Reed, C. A. *Acc. Chem. Res.* **2005**, *38*, 235−242.
(29) Sun, Y.; Drovetskaya, T.; Bolskar, R. D.; Bau, R.; Boyd, P. D. W.; Reed, C. A. *J. Org. Chem.* **1997**, *62*, 3642−3649.
(30) Kubo, Y.; Sugasaki, A.; Ikeda, M.; Sugiyasu, K.; Sonoda, K.; Ikeda, A.; Takeuchi, M.; Shinkai, S. *Org. Lett.* **2002**, *4*, 925−928.
(31) Dudic, M.; Lhoták, P.; Stibor, I.; Petrícková, H.; Lang, K. *New. J. Chem.* **2004**, *28*, 85−90.
(32) Gutsche, C. D. *Calixarenes Revisited*; Royal Society of Chemistry: London, 1998; p 233.
(33) Arimura, T.; Nishioka, T.; Suga, Y.; Murata, S.; Tachiya, M. *Mol. Cryst. Liq. Cryst. Sci. Technol., Sect. A* **2002**, *379*, 413−418.

(34) Konarev, D. V.; Kovalevsky, A. Y.; Li, X.; Neretin, I. S.; Litvinov, A. L.; Drichko, N. y. V.; Slovokhotov, Y. L.; Coppens, P.; Lyubovskaya, R. N. *Inorg. Chem.* **2002**, *41*, 3638−3646.
(35) Litvinov, A. L.; Konarev, D. V.; Kovalevsky, A. Y.; Neretin, I. S.; Coppens, P.; Lyubovskaya, R. N. *Cryst. Growth Des.* **2005**, *5*, 1807−1819.
(36) Hasobe, T.; Imahori, H.; Fukuzumi, S.; Kamat, P. V. *J. Phys. Chem. B* **2003**, *107*, 12105−12112.
(37) Hasobe, T.; Kamat, P. V.; Troiani, V.; Solladie, N.; Ahn, T. K.; Kim, S. K.; Kim, D.; Kongkanand, A.; Kuwabata, S.; Fukuzumi, S. *J. Phys. Chem. B* **2005**, *109*, 19−23.
(38) Imahori, H.; Fujimoto, A.; Kang, S.; Hotta, H.; Yoshida, K.; Umeyama, T.; Matano, Y.; Isoda, S.; Isosomppi, M.; Tkachenko, N. V.; Lemmetyinen, H. *Chem.−Eur. J.* **2005**, *11*, 7265−7275.
(39) Imahori, H.; Mitamura, K.; Shibano, Y.; Umeyama, T.; Matano, Y.; Yoshida, K.; Isoda, S.; Araki, Y.; Ito, O. *J. Phys. Chem. B* **2006**, *110*, 11399−11405.
(40) Imahori, H.; Tkachenko, N. V.; Vehmanen, V.; Tamaki, K.; Lemmetyinen, H.; Sakata, Y.; Fukuzumi, S. *J. Phys. Chem. A* **2001**, *105*, 1750−1756.
(41) Vehmanen, V.; Tkachenko, N. V.; Imahori, H.; Fukuzumi, S.; Lemmetyinen, H. *Spectrochim. Acta A* **2001**, *57*, 2229−2244.
(42) Tkachenko, N. V.; Lemmetyinen, H.; Sonoda, J.; Ohkubo, K.; Sato, T.; Imahori, H.; Fukuzumi, S. *J. Phys. Chem. A* **2003**, *107*, 8834−8844.
(43) Chukharev, V.; Tkachenko, N. V.; Efimov, A.; Guldi, D. M.; Hirsch, A.; Scheloske, M.; Lemmetyinen, H. *J. Phys. Chem. B* **2004**, *108*, 16377−16385.
(44) Chukharev, V.; Tkachenko, N. V.; Efimov, A.; Lemmetyinen, H. *Chem. Phys. Lett.* **2005**, *411*, 501−505.
(45) Armaroli, N.; Marconi, G.; Echegoyen, L.; Bourgeois, J. P.; Diederich, F. *Chem.−Eur. J.* **2000**, *6*, 1629−1645.
(46) Guldi, D. M.; Hirsch, A.; Scheloske, M.; Dietel, E.; Troisi, A.; Zerbetto, F.; Prato, M. *Chem.−Eur. J.* **2003**, *9*, 4968−4979.
(47) Bonifazi, D.; Scholl, M.; Song, F. Y.; Echegoyen, L.; Accorsi, G.; Armaroli, N.; Diederich, F. *Angew. Chem., Int. Ed.* **2003**, *42*, 4966−4970.
(48) Armaroli, N.; Accorsi, G.; Song, F. Y.; Palkar, A.; Echegoyen, L.; Bonifazi, D.; Diederich, F. *ChemPhysChem* **2005**, *6*, 732−743.
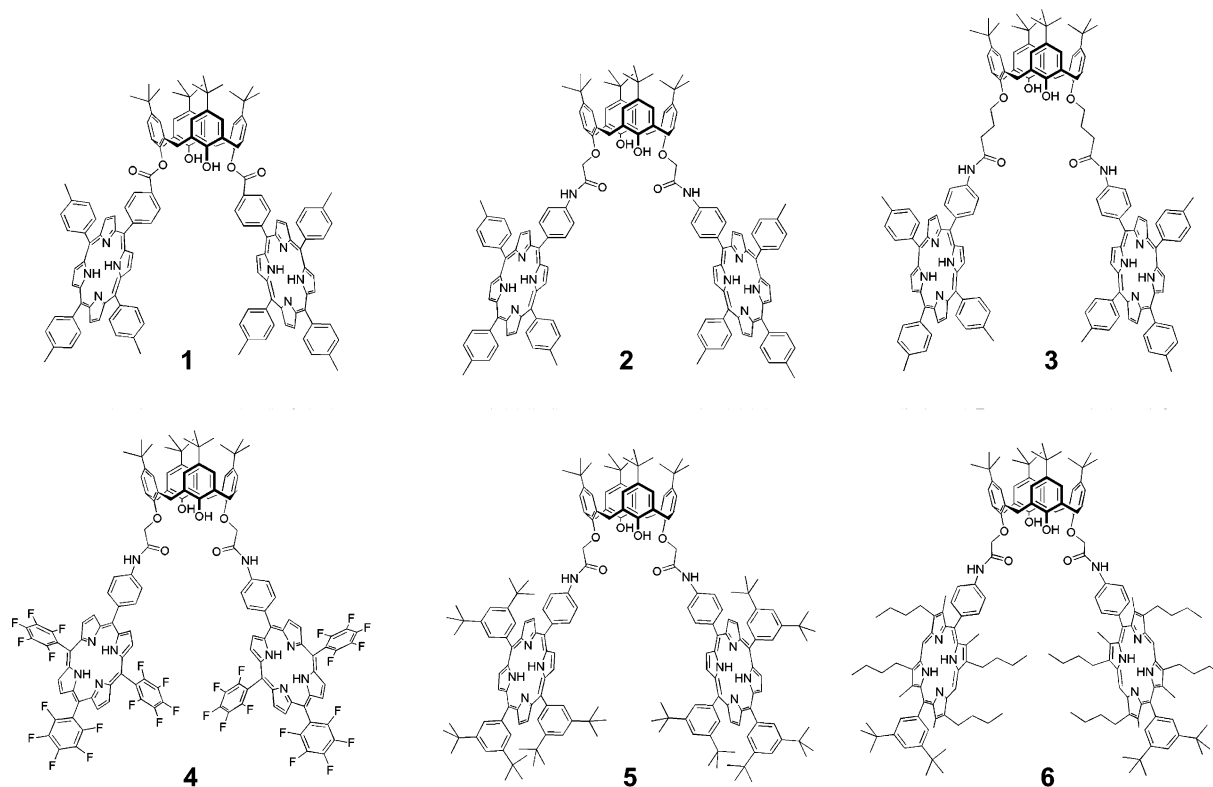(49) Tashiro, K.; Aida, T. *J. Incl. Phenom. Macro. Chem.* **2001**, *41*, 215−217.

Figure 2. Bisporphyrin hosts **1**−**6**.

direct linkage of the porphyrin to a phenolic residue via esterification. *p*-Tolyl substituents on the porphyrin were chosen for solubility reasons and for convenient ¹H NMR identification purposes. Compound **2** extends the linkage by one methylene group and switches the ester to an amide. Compound **3** is the three-methylene analogue of **2**. Despite extensive effort, we have been unable to develop a method to produce the compound with two methylene groups. Compounds **4** and **5** are analogues of the one-methylene compound **2** having pentafluorophenyl and 3,5-*tert*-butylphenyl substituents on the porphyrin meso positions. Similarly, compound **6** replaces the tetraarylporphyrin in **2** with an octaalkyl diaryl porphyrin.

The esterification linkage reaction to produce compound **1** was only achieved in low yield despite several variations in the methodology. The amide linkages in compounds **2**−**6** were all carried out in good yield using dicyclohexylcarbodiimide (DCC) coupling. The monosubstituted tetrarylporphyrins were all prepared by standard methods, and the conjugates **1**−**6** were routinely prepared in 50−100 mg quantities with 50−60% yields. Purification was readily achieved via silica gel column chromatography.

Compounds **1**−**6** were chosen as synthetic targets based on molecular modeling, in a manner similar to our earlier work on Pd-linked bisporphyrins.[19] These calculations indicated that in the trans-linked, lower-rim, bisporphyrins the calixarenes would adopt the commonly observed "pinched cone" conformation. This is borne out experimentally in the ¹H NMR spectra of these compounds where the methylene groups in the calixarenes show AB patterns with J_{HH} = 13.2−13.4 Hz, typical of this conformation.[50]

---

(50) Ostaszewski, R.; Stevens, T. W.; Verboom, W.; Reinhoudt, D. N.; Kaspersen, F. M. *Recl. Trav. Chim. Pays-Bas* **1991**, *110*, 294−298.
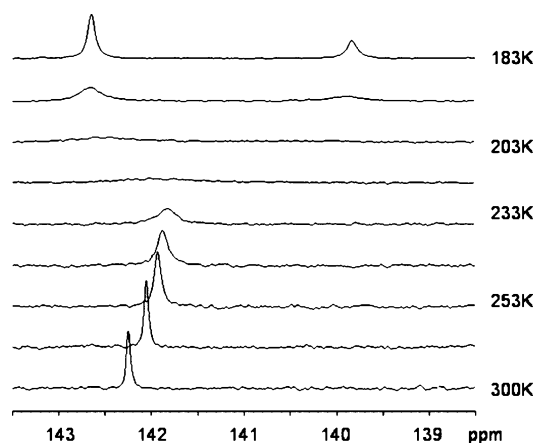

Figure 3. Variable-temperature ¹³C NMR spectrum of ¹³C-enriched C₆₀ in the presence of 0.3 equiv of **2** in toluene-d_8.

The 1:1 complexation of C₆₀ with a bisporphyrin host was easily established for compound **1** because the 1:1 adduct precipitates immediately upon mixing toluene solutions of host and guest. Moreover, the complex remains intact as the major ion in MALDI mass spectrometry, [**1** + C₆₀ + H]⁺ = 2734. The precipitate can be dissolved in chloroform, and from the relative intensities of the porphyrin Soret band and the C₆₀ UV bands, the 1:1 stoichiometry was confirmed. For **2**, **4**, and **5**, 1:1 complexation was established via ¹³C NMR spectroscopy by previously reported methods.[19] As shown in Figure 3, a 3:1 mixture of ¹³C-enriched C₆₀ and **2** in toluene-d_8 shows a single resonance for C₆₀ at 300 K due to time averaging of bound and unbound C₆₀. Upon cooling, this peak broadens and at 183 K splits into separate signals for bound (139.7 ppm) and unbound (142.6 ppm) C₆₀ in a ratio of 2:1. The same behavior was
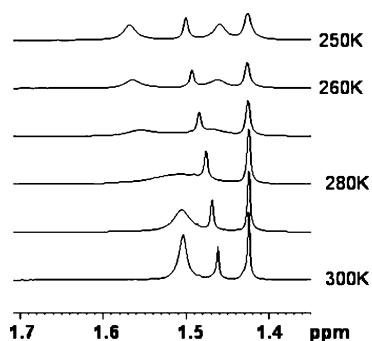
Figure 4. Variable-temperature ^{1}H NMR spectrum in the *t*-butyl region of **5** in the presence of 3 equiv of ^{13}C-enriched C_{60} in toluene-d_8.
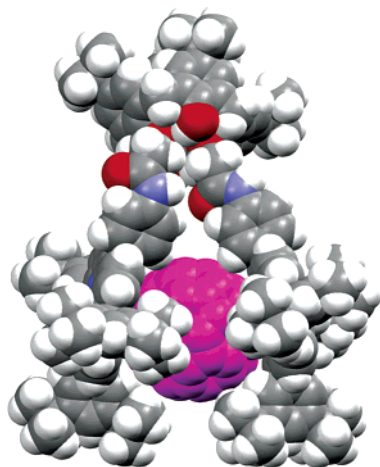

Figure 5. Molecular modeling structure of **5**·C_{60} showing the close approach of the 10,20-*tert*-butylphenyl substituents to C_{60} and the more distant approach of the 15-*tert*-butylphenyl substituent.

Table 1. Binding Constants for Fullerenes of **1**–**6** and Metalated Derivatives of **5** in Toluene

		K, C_{60} (M^{-1})	K, C_{70} (M^{-1})
1	H2	2000 ± 90^a	
2	H2	8700 ± 300^a	38600 ± 500^b
3	H2	2900 ± 300^a	
4	H2	7000 ± 1600^b	13000 ± 6000^b
5	H2	26000 ± 4000^b	234000 ± 20000^b
	Zn(II)	19000 ± 800^b	207000 ± 25000^b
	Cu(II)	11000 ± 1700^b	120000 ± 9000^b
	Ni(II)	14000 ± 3000^b	53000 ± 27000^b
6	H2	2570 ± 24^a	

[a] Fluorescence (295 K). [b] UV−visible (298 K).

dominant ions arising from toluene−acetonitrile solutions were 2+ ions of the 1:1 complexes.

Fullerene Binding Constants in Toluene. The binding constants of **1**, **2**, and **3** for C_{60} and C_{70} were measured by fluorescence quenching titration in toluene and are listed in Table 1. The reliability of these measurements was confirmed for **2** by following fullerene binding in the ^{1}H NMR spectrum. The internal N−H protons of the porphyrin at −2.17 ppm are shifted upfield by the ring current of the fullerene and, under fast exchange conditions at room temperature, provide an alternate measurement of the binding constant. The values agreed within 300 M^{-1}. Compound **2** has a significantly higher binding constant for C_{60} (8700 M^{-1}) than commonly observed in acyclic systems, and it is also larger than the value observed in the phenyl analogue (4920 M^{-1}).[31] It is intriguing that the subtle change of phenyl for *p*-tolyl in three of the peripheral porphyrin substituents in **2** leads to a near doubling of the binding constant. This led us to investigate the effect of substituent variation on the porphyrin in compounds **4**−**6**.

Compounds **4** and **5** show the effect of pentafluorophenyl and 3,5-di-*tert*-butylphenyl substituents in place of tolyl in **2**. In addition, an octaalkylporphyrin derivative, **6**, was prepared. The binding constants for C_{60} and C_{70} were measured by UV−vis titration and are listed in Table 1. The 3,5-di-*tert*-butylphenyl substituents in **5** give rise to the highest binding constant for both C_{60} and C_{70}. From crystal structures of pentafluorophenyl porphyrin/fullerene cocrystallates,[51,52] weak attractive *ortho*-C−F···C_{60} interactions have been identified that might be expected to increase the binding constant of **4** versus that of **2**. However, this is not seen; they have slightly lower binding constants for C_{60} and for C_{70}. From crystallography, 3,5-di-*tert*-butylphenyl groups also appear to have a weak attractive interaction to fullerene,[19] and **5** does show considerable enhancement of fullerene binding relative to **2**. This lack of predictability suggests that differential solvation energies play a major role in dictating affinities, and this idea is supported by the solvent variation studies discussed below.

Compound **6**, with octaalkyl substituents and only two phenyl substituents, shows the lowest binding constant for C_{60}. This may be due to competition from porphyrin−porphyrin face-to-face association, a commonly observed structural motif in less sterically face-hindered porphyrins.

A pyrrolidine-derivatized C_{60}, *N*-methyl-2-phenyl-3,4-fulleropyrrolidine,[53] was compared with C_{60} for binding to **5**. As

observed for **4** and **5**. The upfield shifts of the fullerene in the bound states are the result of ring currents effects of the porphyrin π system on the fullerene. A reciprocal ring current effect of C_{60} on the porphyrin is seen on the internal porphyrin N−H groups.[19] The free-base ^{1}H chemical shift of the free base at −2.0 ppm moves to −2.3 ppm upon complexation of C_{60}.

The proximity of the ortho-C−F bonds of the porphyrin to the bound fullerene in **4**·C_{60} is reflected in the downfield shift of their ^{19}F resonances relative to free base **4**, whereas the meta and para signals show insignificant shifts. Similarly, there is a downfield shift of the *t*-butyl methyl groups in the ^{1}H NMR spectrum of **5**·C_{60} relative to free base **5**. At low temperatures, where free rotation of the 3,5-*tert*-butylphenyl groups at the 10 and 20 positions is slow on the NMR time scale, separate ^{1}H signals are seen for the *t*-butyl groups on each face of the porphyrin (Figure 4). The downfield signal at 1.56 ppm is assigned to the *t*-butyl groups in close proximity to C_{60}; the upfield signal at 1.45 ppm is assigned to *t*-butyl groups exterior to the host cavity, and a signal at 1.42 ppm is assigned to the *t*-butyl groups on the freely rotating phenyl group at the 15 position. As seen in Figure 5, the "jaws" shape of the bisporphyrin host places the 10,20-phenyl groups closer to the fullerene guest than the 15-phenyl group, leading to face discrimination of the *t*-butyl groups at the 10,20 positions but not the 15.

The 1:1 stoichiometry of binding of both C_{60} and C_{70} to **5** was also established by electrospray mass spectrometry. The

(51) Hosseini, A.; Hodgson, M. C.; Tham, F. S.; Reed, C. A.; Boyd, P. D. W. *Cryst. Growth Des.* **2006**, *6*, 397−403.
(52) Olmstead, M. M.; Nurco, D. J. *Cryst. Growth Des.* **2006**, *6*, 109−113.
(53) Prato, M.; Maggini, M. *Acc. Chem. Res.* **1998**, *31*, 519−526.

Table 2. Binding Constants for Fullerenes of **5** as a Function of Solvent

	C_6H_{12}	C_6H_5CN	CH_2Cl_2	toluene	CH$_3$CN/ toluene 1:19	CH$_3$CN/ toluene 1:9	CH$_3$CN/ toluene 1:3	CH$_3$CN/ toluene 1:1
solubility (mg/mL)	0.036	0.41	0.25	2.60	0.920	0.710	0.267	0.031
log K	6.61	4.69	4.91	4.42	4.61	4.85	5.26	6.28

expected for a fullerene where the addend has only a small steric and electronic influence, the binding constant, 6000 M^{-1}, was smaller but comparable.

Previous studies of the role of porphyrin metalation in controlling fullerene binding constants have shown somewhat variable trends.[28] As shown in Table 1 for C$_{60}$ and C$_{70}$ binding to **5**, the affinities of metalloporphyrins are all lower than those of the corresponding free base. This tendency has been observed with most but not all porphyrin hosts. A subtle interplay of differential solvation energies and metalloporphyrin–fullerene interaction energies is believed to control these binding constants.[28]

The most recent theoretical analysis of porphyrin–fullerene interaction energies[54] shows the need for detailed experimental studies on the energetics of binding and the role of the solvent. Only with studies of this kind will a separation of solvation versus intrinsic binding effects become possible. For this reason, we have explored the solvent and temperature dependence of fullerene binding constants for **2** and **5**.

Solvent Dependence of Binding Constants. The influence of solvent on the supramolecular host–guest interaction is pronounced. The energetics of binding can conceptually be broken down into desolvation of the individual host and guest, intrinsic binding affinities, and resolvation of the host–guest complex. The formation of a host–guest complex will be favored in solvents in which either or both of the host–guest components are weakly solvated or in which the solvation free energy of the complex exceeds that of the components. Traditionally, the consideration for the choice of solvents for titration of a host with a fullerene has been limited by the solubility of fullerenes in organic solvents. The solubility of C$_{60}$ increases in the order: benzene (1.70 mg/mL) < toluene (2.80 mg/mL) < *p*-xylene (3.14–5.90 mg/mL) < chlorobenzene (5.7–7.0 mg/mL) < CS$_2$ (7.7–7.9 mg/mL) ≪ *o*-dichlorobenzene (13.8–27.0 mg/mL).[55] Haino and co-workers studied the solvent effect on the association of both C$_{60}$ and C$_{70}$ with mono- and biscalix[5]arenes.[56–58] The association constants decrease in the order: toluene > benzene > CS$_2$ > *o*-dichlorobenzene. With the apparent exception of toluene, the association constant decreases with increasing solubility of the fullerene. Aida and Tashiro have investigated the competition between complexation and solvation in C$_{120}$ complexes of a cyclic bisporphyrin.[59] Again, the association constant for the fullerene decreases in

the order: toluene > chlorobenzene > dichlorobenzene. This follows the solubility order for fullerenes and is consistent with dominance of the fullerene desolvation energy in determining relative magnitudes of the binding constants.

Bisporphyrin **5** was chosen for solvent-dependent studies because it has the highest binding constant for C$_{60}$ and C$_{70}$ in toluene compared with other hosts. In addition, it is soluble in a range of organic solvents. As shown in Table 2, titration of a concentrated solution of C$_{60}$ in toluene into a dilute solution of **5** in benzonitrile showed an increase in the binding constant to 50 000 M^{-1}, compared to 25 000 M^{-1} in toluene. Similar titrations in dichloromethane afforded an association constant of 90 000 M^{-1}. More dramatically, titrations carried out in cyclohexane showed an increase in binding constant to 4 000 000 M^{-1}. The relative solubility of C$_{60}$ decreases in the order: toluene > benzonitrile > dichloromethane ≫ cyclohexane, again suggesting that desolvation of the fullerene is the dominant factor determining the energetics of host–guest formation.

Mixtures of acetonitrile/toluene provide an interesting option for the control of the association constant because the solubility of C$_{60}$ decreases in a nonlinear fashion over a large range as the v/v % of acetonitrile increases.[55] A solution of **5** in a mixture of acetonitrile/toluene was prepared such that the solubility of C$_{60}$ at 1:1 v/v solvent ratio (0.031 mg/mL) was comparable to that in cyclohexane (0.036 mg/mL). The absorption spectrum of this mixture shows no evidence of cluster formation as has been found in solutions of porphyrins and fullerenes in higher ratios of acetonitrile, where broad intense absorptions are observed in the visible and near-infrared regions relative to the spectra of the parent porphyrin and fullerene.[36] In this case, the binding constant was of the same order of magnitude (1 000 000 M^{-1}) as the binding constant in cyclohexane. At lower ratios of acetonitrile (1:3, 1:9, and 1:19), where the solubility of C$_{60}$ ranges from 0.267 to 0.920 mg/mL, the decrease in binding constant is very significant (Figure 6). The essential linearity of the plot of log K versus C$_{60}$ solubility is intriguing because the correlation between binding constant and solvent composition implies a direct correlation of binding constant with the C$_{60}$ solvation energy. These data continue to support the idea that desolvation of the fullerene is the dominant contributor to the energetics of fullerene binding in solution.

Enthalpy and Entropy of Fullerene Binding. The temperature dependence of the binding constant (K) of **2** with C$_{60}$ was measured at six different temperatures using ^{1}H NMR titration spectroscopy in toluene-d_8. The association of C$_{70}$ with **2** in toluene is sufficiently large to allow the determination of the thermodynamics of binding by UV–vis spectroscopy. The enthalpy (ΔH) and entropy (ΔS) of complex formation with C$_{60}$ and C$_{70}$ with **2** were evaluated by a van't Hoff plot of ln-(K) versus $1/T$. As illustrated for C$_{60}$ in Figure 7, these van't Hoff plots are linear with a positive slope. This indicates that the formation of these host–guest complexes is exothermic and

(54) Jung, Y.; Head-Gordon, M. *Phys. Chem. Chem. Phys.* **2006**, *8*, 2831–2840.
(55) Beck, M. T.; Mandi, G. *Fullerene Sci. Technol.* **1997**, *5*, 291–310.
(56) Haino, T.; Yanase, M.; Fukazawa, Y. *Angew. Chem., Int. Ed.* **1998**, *37*, 997–998.
(57) Yanase, M.; Matsuoka, M.; Tatsumi, Y.; Suzuki, M.; Iwamoto, H.; Haino, T.; Fukazawa, Y. *Tetrahedron Lett.* **2000**, *41*, 493–497.
(58) Haino, T.; Yanase, M.; Fukunaga, C.; Fukazawa, Y. *Tetrahedron* **2006**, *62*, 2025–2035.
(59) Tashiro, K.; Hirabayashi, Y.; Aida, T.; Saigo, K.; Fujiwara, K.; Komatsu, K.; Sakamoto, S.; Yamaguchi, K. *J. Am. Chem. Soc.* **2002**, *124*, 12086–12087.
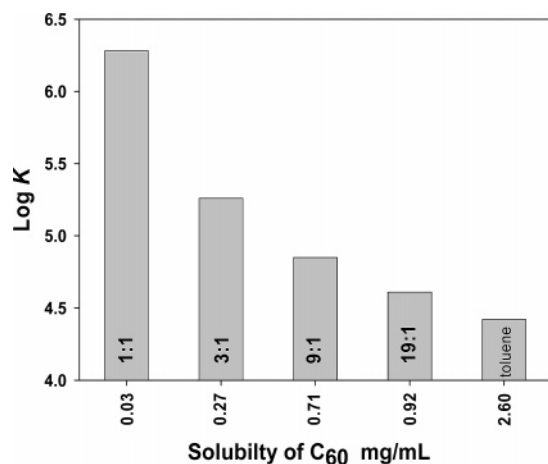
Figure 6. Variation of the binding constant for C_{60} (log K) with **5** as a function of fullerene solubility in toluene/acetonitrile solvent mixtures (v/v %).
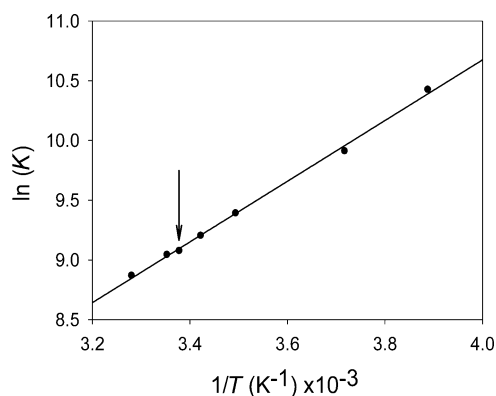

Figure 7. Plot of ln(K) versus $1/T$ for the binding of C_{60} with **2**. The arrow indicates a value of K determined from a fluorescence titration.

enthalpy driven. The enthalpy of binding for C_{70} is higher by 4 kJ mol^{-1}, which correlates with the higher binding constant of C_{70} relative to that of C_{60}. The entropies of formation are small and positive (Table 3), indicating a small entropic contribution to the binding energies. This indicates that the negative entropy contribution expected from an associative reaction is countered by an increase in solvent disorder upon complexation compared to the individual fullerene and porphyrin components.

Similar measurements for C_{60} with **5** in both toluene and cyclohexane again gave linear van't Hoff plots with positive slopes, indicating enthalpy-driven complex formation. The ΔH and ΔS values for C_{60} with **5** in toluene are both somewhat larger in magnitude than those found for **2** (see Table 3). These increases rationalize the trebling of the binding constant of **5·**C_{60} relative to **2·**C_{60}. On the other hand, for **5·**C_{60} in cyclohexane, ΔH doubles in magnitude relative to that in toluene and ΔS is small but negative. The increase in ΔH is sufficiently large that the unfavorable entropy change is overcome *and* the binding constant increases by a factor of ca. 100. This can be understood in terms of the poor solvation of a fullerene by cyclohexane relative to toluene.

Absorption and Luminescence Spectra: Ground and Excited State CT Interactions. The absorption spectra of the receptor molecules **5** and **Zn₂5** in cyclohexane are reported in Figure 8. They are characterized by the typical Soret and Q-bands in the visible spectral region, with molar extinction coefficients approximately twice as intense as in those of regular

free-base and Zn tetraphenylporphyrins.[60,61] This suggests little or no interaction between porphyrin macrocycles in **5** and **Zn₂5**.

The absorption spectra of solutions containing the fullerene adducts are shown in Figure 9. Adduct formation is clearly signaled by the substantial intensity decrease (−40%) and red shift (9 nm) of the porphyrin Soret bands (either free-base or Zn-type) compared to the receptors alone, and the appearance of new and weak absorption bands above 700 nm is attributable to ground state porphyrin-to-fullerene charge transfer (CT) interactions. Similar low-energy bands have been observed in previously investigated face-to-face porphyrin−fullerene conjugates.[44,45,47]

The CT absorption bands of the adducts with a free-base porphyrin are at shorter wavelength (around 720 nm) relative to those involving the corresponding Zn-porphyrin receptor (ca. 780 nm). This is a consequence of the lower oxidation potential of Zn-porphyrins.[44]

Within the same receptor, the CT band tends to shift to lower energy with C_{70} relative to C_{60}, reflecting the slightly lower reduction potential of C_{70} compared to that of C_{60}.[62] Notably, in the present four adducts where the carbon sphere is sandwiched between two porphyrin units, CT bands show a pronounced shoulder with molar extinction coefficient of the order of ca. 3000 M^{-1} cm^{-1}, a value substantially higher than that exhibited in similarly apolar toluene solution by conjugates having just one porphyrin donor moiety for the fullerene acceptor (50 M^{-1} cm^{-1}).[45]

A direct relationship between supramolecular binding of the fullerenes to a bisporphyrin host and the appearance of a NIR band can be demonstrated with **Zn₂5·**C_{60}, where the component absorptions are well separated and solubility is high. Titration of a solution of C_{60} into a concentrated solution of Zn₂5 (3 × 10^{-5} M) correlates with the appearance of a new absorption band at ~770 nm (Figure 10). A least-squares fit of the increase in the intensity of the 770 nm band as a function of C_{60} concentration gave a formation constant of 21,900 ± 2700 M^{-1} at 296 K, comparable to the binding constant obtained independently by UV−vis titration (19,390 ± 800 M^{-1} at 298 K).

Evidence that this NIR band is a porphyrin-to-fullerene charge transfer (CT) in origin is obtained by systematic variation of the porphyrin. The energy of this band increases for C_{60} in order: **Zn₂5** < **Cu₂5** < **5** < **Ni₂5**. This correlates with the lower lying energy of the HOMO of the porphyrin as calculated by DFT methods. As illustrated in Figure 11, the lower the energy of the porphyrin HOMO, the greater the gap to the fullerene LUMO. The CT band is not observed in **4·**C_{60} presumably because the electron-withdrawing fluoro substituents increase the energy of this band into the visible region, where it is masked by the more intense Q-bands of the porphyrin. Indeed, a broadening of the porphyrin bands in the visible region is apparent, but deconvolution cannot be reliably carried out.

Fluorescence spectra of the receptor molecules **5** and **Zn₂5** in cyclohexane are depicted in the inset of Figure 8; spectral shapes, fluorescence quantum yields, and related singlet lifetimes (Table 4) are in line with monomeric tetraphenylporphyrins.[60,61]

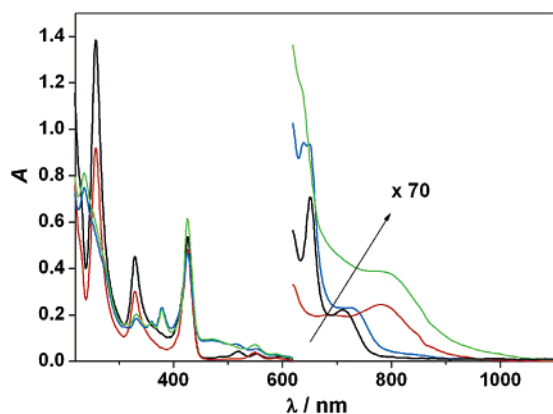(60) Flamigni, L.; Armaroli, N.; Barigelletti, F.; Balzani, V.; Collin, J. P.; Dalbavie, J. O.; Heitz, V.; Sauvage, J. P. *J. Phys. Chem. B* **1997**, *101*, 5936−5943.
(61) Flamigni, L.; Barigelletti, F.; Armaroli, N.; Collin, J. P.; Sauvage, J. P.; Williams, J. A. G. *Chem.−Eur. J.* **1998**, *4*, 1744−1754.
(62) Xie, Q. S.; Perez-Cordero, E.; Echegoyen, L. *J. Am. Chem. Soc.* **1992**, *114*, 3978−3980.
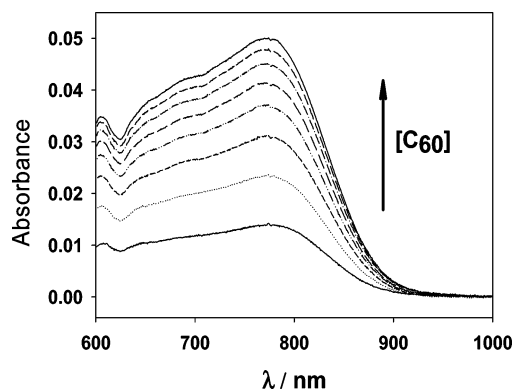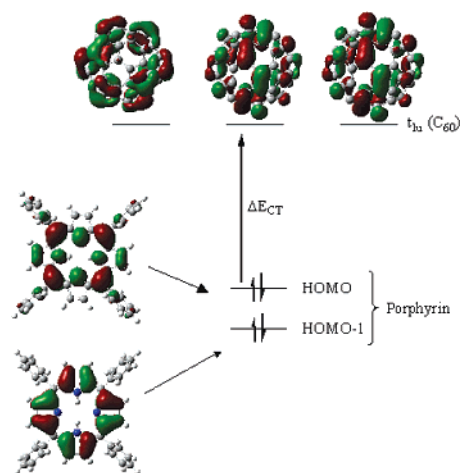
Table 3. Thermodynamic Parameters for the Binding of Fullerenes to **2** and **5**

	2				5			
	C₆₀ Toluene		C₇₀ Toluene		C₆₀ Toluene		C₆₀ Cyclohexane	
ΔH_c kJ mol^{-1}	ΔS_c J K^{-1} mol^{-1}	ΔH_c kJ mol^{-1}	ΔS_c J K^{-1} mol^{-1}	ΔH_c kJ mol^{-1}	ΔS_c J K^{-1} mol^{-1}	ΔH_c kJ mol^{-1}	ΔS_c J K^{-1} mol^{-1}
-21 ± 1.5	4.5 ± 4.9	-25 ± 2.1	4.1 ± 6.6	-22.7 ± 4.1	8.3 ± 14.9	-40.3 ± 8	-8.4 ± 12
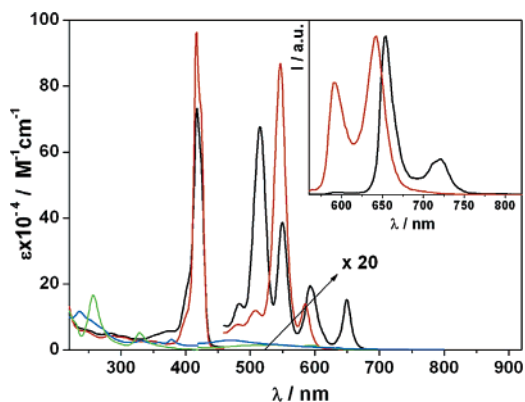
Figure 8. Electronic absorption spectra of **5** (black), **Zn₂5** (red), C₆₀ (green), and C₇₀ (blue) in cyclohexane; the spectral window above 420 or 460 nm has been multiplied by a factor of 20. Inset: Fluorescence spectra of **5** (black) and **Zn₂5** (red) (λ_{exc} = 425 nm, o.d. = 0.1, cyclohexane).

Figure 10. NIR−UV−vis spectrum of titration of **Zn₂5** with C₆₀ in toluene (**Zn₂5** spectrum subtracted). [C₆₀]:[**Zn₂5**] = 1:2, 1:1, 3:2, 4:2, 5:2, 6:2, 7:2, 8:2.

Figure 9. Electronic absorption spectra of solutions containing **5**/C₆₀ (black), **5**/C₇₀ (blue), **Zn₂5**/C₆₀ (red), and **Zn₂5**/C₇₀ (green) in cyclohexane; the spectral window above 620 nm has been multiplied by a factor of 70. Details on the preparation of these samples, which contain a concentration of the supramolecular adduct of about 1.0×10^{-6} M and an excess of C₆₀ or C₇₀ (ca. 5 times higher), are given in the Experimental Section.

Figure 11. Illustrations of the HOMO and LUMO of a tetraphenylporphyrin·C₆₀ complex and a schematic representation of the energy levels of the frontier orbitals.

Upon predominant excitation of the porphyrin moieties within the supramolecular adducts **5**·C₆₀, **5**·C₇₀, **Zn₂5**·C₆₀, and **Zn₂5**·C₇₀ (425 nm, Soret band), dramatic quenching of the porphyrin fluorescence is observed (Table 4). The residual fluorescence in **5**·C₆₀ and **Zn₂5**·C₆₀ is mainly attributable to some amount of unbound porphyrin receptor (see Experimental Section); this is confirmed by the lifetime values, which are identical to those of the reference molecules. The residual porphyrin emission turns out to be 10 times weaker in the adducts with C₇₀, and this is consistent with the higher association constants observed with the larger carbon cage. For **5**·C₇₀, a short lifetime component was observed, which is attributed to the quenched free-base porphyrin within the adduct.

By recording the emission spectra of **5**·C₆₀, **5**·C₇₀, **Zn₂5**·C₆₀, and **Zn₂5**·C₇₀ down to the NIR region, low-energy bands attributable to charge transfer emissive states are detected with lifetimes shorter than 1 ns (Table 5).[45,48]

Table 4. Porphyrin Fluorescence and Lifetime Data in Cyclohexane Solution

	λ_{em} (%)^{a,b} (nm)	Φ_{em} (%)^a	τ^c (ns)
5	654	5.2	10.2
Zn₂5	592	2.3	2.4
5·C₆₀	654	0.4	10.1^d
Zn₂5·C₆₀	592	0.3	2.4^d
5·C₇₀	654	0.04	0.6^e−9.8^d
Zn₂5·C₇₀	592	0.03	2.4^d

^{a} λ_{exc} = 425 nm, Soret band. ^{b} Highest energy emission feature. ^{c} λ_{exc} = 407 nm, laser diode. ^{d} Residual fluorescence from some unbound receptor (see text). ^{e} Shorter component attributable to quenching of the porphyrin in the adduct.

Emission maxima are at higher energy for **5**·C₆₀ and **5**·C₇₀ (Figure 12) compared to **Zn₂5**·C₆₀ and **Zn₂5**·C₇₀ (Figure 13), in line with the CT absorption trends. In the case of **5**·C₆₀ and **5**·C₇₀, a tail of residual porphyrin fluorescence has been removed to obtain the profiles depicted in Figure 12. Emission maxima

Table 5. CT Luminescence and Lifetime Data at 298 K in Cyclohexane

	$\lambda_{max}{}^{a}$ (nm)	τ^{c} (ns)
5·C$_{60}$	848 840^{b}	0.6
5·C$_{70}$	876 866^{b}	0.6
Zn$_2$5·C$_{60}$	982 962^{b}	≤0.3^{c}
Zn$_2$5·C$_{70}$	992 972^{b}	≤0.3^{c}

^{a} λ_{exc} = 425 nm. ^{b} Corrected values for the photomultiplier response. ^{c} λ_{exc} = 407 nm, laser diode; close to the lower limit of instrumental time resolution, experimental uncertainty ±50%.
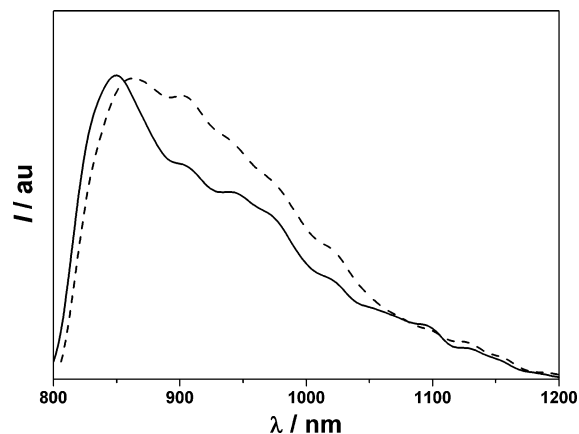
Figure 12. Emission spectra of **5·C$_{60}$** (solid line) and **5·C$_{70}$** (dashed line) in cyclohexane solution (o.d. = 0.5, λ_{exc}= 425 nm). The tail of the porphyrin residual fluorescence has been mathematically subtracted.
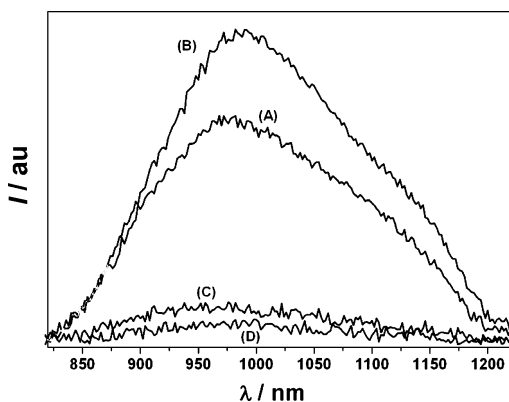
Figure 13. Emission spectra of **Zn$_2$5**/C$_{60}$ (A: o.d. = 0.5, λ_{exc}= 425 nm) and **Zn$_2$5**/C$_{70}$ (B: o.d. = 0.5, λ_{exc}= 425 nm; C: o.d. = 0.07, λ_{exc}= 548 nm; D: o.d. = 0.06, λ_{exc}= 784 nm) in cyclohexane solution.

of C$_{70}$ adducts are slightly bathochromically shifted and, at least in the case of the **Zn$_2$5** receptor where the spectra are well separated from the residual porphyrin fluorescence, relatively more intense than for C$_{60}$ analogues (Figure 13).

By using corrected luminescence spectra and pristine C$_{60}$ in toluene as reference, the emission quantum yield of **Zn$_2$5·C$_{70}$** was estimated to be of the order of 10^{-4}, that is, similar to C$_{60}$−porphyrin conjugates investigated earlier.[48] The low-emission quantum yield is related to the very low energy of the emitting state, according to the energy gap law.[63] Notably, the CT

emission band, tested in the case of the highest signal (**Zn$_2$5·C$_{70}$**), is also detected upon direct excitation in the CT absorption bands (784 nm), although the signal is very weak due very low absorbance and excitation power (Figure 13). This demonstrates that **5·C$_{60}$**, **5·C$_{70}$**, **Zn$_2$5·C$_{60}$**, and **Zn$_2$5·C$_{70}$** have to be considered electron donor/acceptor complexes and not exciplexes since their interaction is not exclusively established in the excited state but also in the ground state.[64]

The CT bands are of interest because information relevant to the rate of photoinduced electron transfer can be obtained from consideration of their energies, bandwidths, extinction coefficients, and inter-chromophore distance. The rate of electron transfer is proportional to the square of the electronic coupling constant V in the Marcus−Hush relationship for the rate of electron transfer k_{ET} (eq 1).[65,66]

$$k_{et} = \left(\frac{4\pi^3}{\hbar^2 \lambda k_B T}\right)^{1/2} V^2 \exp\left[-\frac{(\Delta G_{ET}^{\circ} + \lambda)^2}{4\lambda k_B T}\right] \quad (1)$$

where λ = reorganization energy, ΔG°_{ET} = reaction free energy, k_B = Boltzman constant, $\hbar$ = Planck constant, V = electronic coupling (electronic matrix element), and T = absolute temperature.

The CT bands in the absorption spectra may be used to estimate the electronic coupling (V) between the fullerene and porphyrin using eq 2.[67]

$$V = \frac{2.06 \times 10^{-2}(\epsilon_{max}\nu_{max}\Delta\nu_{1/2})^{1/2}}{R_{cc}} \quad (2)$$

where V = electronic coupling (in cm^{-1}), ϵ_{max} = extinction coefficient of the CT band at maximum (in mol^{-1} cm^{-1}), ν_{max} = frequency of the CT band (in cm^{-1}), $\Delta\nu_{max}$ = full width at half-height (in cm^{-1}), and R_{cc} = porphyrin center to fullerene center distance (in Å); $\Delta\nu_{max}$ was obtained from a Gaussian fit to the lower energy portion of the CT band, and R_{cc} was taken as 6.25 Å, the common value observed in fullerene−porphyrin cocrystallates.[68] The electronic coupling (V) between the bisporphyrin and C$_{60}$ decreases in the order of Cu(II) (790 cm^{-1}) > Zn(II) (760 cm^{-1}) > free base (700 cm^{-1}).

Finally, we address the question of how the CT band is affected by solvent. In a self-associated fullerene−porphyrin dyad, Guldi et al. observed a red shift of 27 nm in energy of the CT band upon increasing the solvent polarity from toluene (ϵ = 2.4) to benzonitrile (ϵ = 26).[46] On the other hand, Chukharev et al. observed no significant difference in either the energy of the CT band or the electronic coupling between the two chromophores upon changing the solvent from toluene (ϵ = 2.4) to cyclohexane (ϵ = 2.0).[43] We find there is no significant shift in energy (ν_{max}) of the CT band in **Zn$_2$5·C$_{60}$** in cyclohexane (778 nm), toluene (772 nm), or benzonitrile (766 nm). This indicates that neither ground state nor the excited state is highly solvated, consistent with the fullerene guest being well encapsulated by the porphyrin host. Nevertheless, the band

(63) Englman, R.; Jortner, J. *Mol. Phys.* **1970**, *18*, 145−164.

(64) Balzani, V.; Scandola, F. *Supramolecular Photochemistry*; Ellis Harwood: Chichester, U.K., 1991; p 248.
(65) Marcus, R. A. *J. Phys. Chem.* **1989**, *93*, 3078−3086.
(66) Marcus, R. A. *Angew. Chem., Int. Ed.* **1993**, *105*, 1161−1172. See also: *Angew. Chem., Int. Ed. Engl.* **1993**, *32*, 1111−1121.
(67) Barbara, P. F.; Meyer, T. J.; Ratner, M. A. *J. Phys. Chem.* **1996**, *100*, 13148−13168.
(68) Boyd, P. D. W.; Hodgson, M. C.; Chaker, L.; Rickard, C. E. F.; Oliver, A. G.; Brothers, P. J.; Bolskar, R.; Tham, F. S.; Reed, C. A. *J. Am. Chem. Soc.* **1999**, *121*, 10487−10495.

widths ($\nu_{1/2}$) vary somewhat, and this leads to some variation in the electronic coupling values, with benzonitrile (830 cm^{-1}) slightly larger than cyclohexane (790 cm^{-1}) or toluene (760 cm^{-1}).

Conclusions

Calix[4]arenes are convenient scaffolds for the construction of bisporphyrins. The easy variation of the covalent linkage at the lower rim allows positional optimization of the two porphyrins for maximal fullerene binding. The attachment of porphyrins via an amide linker with a single methylene spacer (compound **2**) proved to be most suited for the acceptance of a fullerene guest. In addition, fullerene binding is affected by the choice of peripheral substituents on the porphyrin and those on the upper rim of the calixarene.

Systematic studies on the binding constants of fullerene guests into bisporphyrin hosts indicate a strong dependence on differential solvation energies. In particular, the inverse correlation of binding constant with solubility of fullerenes in various solvents shows that the desolvation of the fullerene is a major contributor to the energetics of fullerene binding. The thermodynamics of binding are consistent with an enthalpy-driven, solvation-dependent process, making solvent choice a powerful way to control binding constants.

By showing a direct relationship between supramolecular binding of a fullerene guest to a bisporphyrin host and the appearance of a broad NIR absorption band, whose energy increases with stability of the porphyrin HOMO, the porphyrin-to-fullerene charge transfer nature of this band has been placed on a firm footing.

Experimental Section

General. ^{1}H and ^{13}C NMR spectra were obtained on a Bruker AM-400 spectrometer, and ^{19}F NMR spectra were recorded on a Bruker AM-300 spectrometer. FAB mass spectra were recorded on a VG-70 spectrometer, MALDI-TOF on a PerSeptive Biosystems Voyager-DE STR spectrometer using a dithranol matrix, and electrospray mass spectra on an Agilent Technologies 1956 MSD mass spectrometer. Binding constants were measured by fluorescence quenching titrations on a Hitachi F2000 spectrometer, by UV–vis titration on a Hewlett-Packard 8452 diode array spectrometer with NESLAB RTE 111 water bath. A Perkin-Elmer Lambda 35 UV–vis–NIR spectrometer was used to measure charge transfer bands. NMR spectra were recorded in CDCl$_3$ containing TMS as reference and filtered through K$_2$CO$_3$ to remove traces of HCl. The temperature of the NMR probe and the sample was calibrated using the ^{1}H NMR spectra of dry methanol.

Fluorescence titrations were carried out using stock solutions of bisporphyrins (3 mL) in a quartz cuvette (1 cm path length). The solution was excited at the wavelength of the first Q-band (e.g., excitation λ = 516 nm for **2**), and the fluorescent emission intensity was monitored at the peak recorded from a wavelength scan. C$_{60}$ in toluene was added in 10 μL aliquots and the emission intensity (I) recorded after each addition. A plot of I versus [C$_{60}$] was carried out to yield the binding constant by a nonlinear least-square methods.[69,70]

UV–vis titrations were carried out using stock solutions of bisporphyrins (3 mL) in a quartz cuvette (1 cm path length). The Soret band in the spectrum was monitored at the wavelength recorded for the free bisporphyrin. A concentrated C$_{60}$ solution in toluene was added in 10 μL aliquots to both the blank and sample cells and the absorbance

recorded after each addition. A plot of absorbance (A) versus C$_{60}$ concentration was used to obtain the fullerene binding constant using a nonlinear fitting method.[69]

Spectroscopic Studies. The spectroscopic investigations were carried out in cyclohexane (Carlo Erba spectroscopic grade) in fluorimetric cuvettes with an optical path of 1 cm. Absorption spectra were recorded with a Perkin-Elmer λ9 spectrophotometer. Visible and NIR luminescence spectra were obtained with an Edinburgh FLS920 spectrometer equipped with either a Peltier-cooled Hamamatsu R-928 (vis region) or a supercooled (193 K) Hamamatsu R5509-72 PMT detector (NIR region); in the latter configuration, a TM300 emission monochromator with NIR grating blazed at 1000 nm was used. An Edinburgh Xe900 450 W xenon arc amp was used as light source; the emission calibration curve was supplied by the manufacturer. Emission lifetimes were determined with the single photon counting technique by means of the same Edinburgh FLS920 spectrometer using a laser diode as excitation source (1 MHz, λ_{exc} = 407 nm, 200 ps time resolution after deconvolution) and the above-mentioned PMTs as detectors.

In order to make spectroscopic investigations on the supramolecular adducts, it is necessary to find a balance between two contrasting factors: the need to get a strong fraction of associated receptor and the need to have a relatively low optical density of the solutions for recording spectra under acceptable optical conditions. In light of this and of the association constant of **5** and **Zn$_2$5** with C$_{60}$ in cyclohexane, that is, 2×10^6 M^{-1}, spectroscopic investigations were carried out as follows. Solutions containing a mix of 1.0×10^{-6} M *of* **5** or **Zn$_2$5** and 5.0×10^{-6} M of C$_{60}$ or C$_{70}$ were prepared, obtaining a fraction of associated receptor exceeding 90%. Under these conditions, we get ca. 1.0×10^{-6} M of the supramolecular adducts **5·C$_{60}$**, **5·C$_{70}$**, **Zn$_2$5·C$_{60}$**, and **Zn$_2$5·C$_{70}$**, an excess 4 times more concentrated of the unbound fullerene molecule, and very little concentration of the free receptor ($\leq 10^{-7}$ M). Under these conditions, it is possible to excite, in the adduct, the porphyrin moiety on the very intense Soret band with a >95% selectivity while keeping the optical density at a reasonable value (o.d. = 0.5–0.6) for the detection of weak luminescence signals in the near-infrared spectral region. Spectroscopic experiments by preferential excitation of the fullerene chromophore (e.g., 330 nm for C$_{60}$) were not carried out, given the large unbound excess of the carbon allotrope under the working conditions.

Synthesis. Reactions were carried out in oven-dried glassware under an atmosphere of dry, oxygen-free nitrogen. Analytical grade organic solvents were dried by standard methods.[71] The progress of reactions was monitored by silica gel thin layer chromatography (TLC). The synthesis of the porphyrin and calix[4]arene precursors is detailed in the Supporting Information. C$_{60}$, C$_{70}$, and ^{13}C-enriched C$_{60}$ were purchased from SES RESEARCH, Houston, Texas.

5,11,17,23-Tetra-*tert*-butyl-25,27-di[(4-carboxyphenyl)-10,15,20-tris-(*p*-methylphenyl)porphyrin]-26–28-dihydroxycalix[4]arene, 1. The synthetic procedure is based on the report of Neises and Steylich.[72] TTP-COOH (0.0998 g, 0.142 mmol), *p-tert*-butylcalix[4]arene (0.0458 g, 0.0706 mmol), and DMAP (0.0035 g, 0.0286 mmol) were combined in dry dichloromethane (5 mL), and the mixture was cooled to $\leq$0 °C. DCC (0.0308 g, 0.149 mmol) in dry dichloromethane was added dropwise and the reaction mixture allowed to warm to room temperature followed by stirring overnight under dinitrogen gas. Precipitated urea was removed by filtration through celite, and precipitated porphyrin product(s) were washed through the celite with chloroform. The filtrate solvent was removed in vacuo and the resulting residue dissolved in chloroform and filtered once more to remove the last traces of urea. Silica gel was added to the filtrate and solvent removed in vacuo to adsorb the porphyrin products on to the gel in preparation for column chromatography. Elution with dichloromethane/*n*-hexane (3:1) produced the first band, which was further purified by preparative layer

(69) Bourson, J.; Pouget, J.; Valeur, B. *J. Phys. Chem.* **1993**, *97*, 4552–4557.
(70) Encinas, S.; Bushell, K. L.; Couchman, S. M.; Jeffery, J. C.; Ward, M. D.; Flamigni, L.; Barigelletti, F. *J. Chem. Soc., Dalton Trans.* **2000**, 1783–1792.
(71) Riddick, J. A.; Bunger, W. B. *Organic Solvents: Physical Properties and Methods of Purification*; Wiley: New York, 1986.
(72) Neises, B.; Steglich, W. *Angew. Chem., Int. Ed. Engl.* **1978**, *17*, 522–524.

chromatography (plc) eluting with toluene/*n*-hexane (3:1). The slower moving of the two major plc bands was extracted from the silica gel with dichloromethane and solvent removed in vacuo to give the desired product as a purple residue (0.0043 g, 3%). ^{1}H NMR (C$_6$D$_6$): δ = -2.89 (s, 4 H, $-$N*H*$-$), 1.15 (s, 18 H, $-$C(C*H*$_3$)$_3$), 1.35 (s, 18 H, $-$C(C*H*$_3$)$_3$), 2.18 (s, 12 H, $-$C*H*$_3$), 2.50 (s, 6 H, $-$C*H*$_3$), 3.71 (d, *J* = 14 Hz, 4 H, $-$C*H*$_2-$), 4.51 (d, *J* = 14 Hz, 4 H, $-$C*H*$_2-$), 6.45 (d, *J* = 7.6 Hz, 8 H), 6.56 (d, *J* = 7.2 Hz, 8 H), 7.34 (d, *J* = 7.6 Hz, 4 H), 8.03 (d, *J* = 4.8 Hz, 4 H), 8.08 (d, *J* = 8.0 Hz, 4 H), 8.25 (d, *J* = 4.8 Hz, 4 H), 8.36 (d, *J* = 7.6 Hz, 4 H), 8.55 (d, *J* = 4.8 Hz, 4 H), 8.82 (d, *J* = 4.4 Hz, 4 H), 9.00 (d, *J* = 8.4 Hz, 4 H) ppm. HR FAB-MS: calcd for [M$^+$] *m/z* = 2012.96438; found 2012.96265. UV/vis (toluene): λ_{max} = 417 (ϵ_{max} = 530 000), 520 (29 000), 555 (19 000), 594 (11 000), 650 nm (8600 L·mol^{-1}·cm^{-1}).

General Procedure for Coupling of Monoaminoporphyrins (*p*-MAP) with Calix[4]arene. A solution of 25,27-dicarboxy-26$-$28-dihydroxycalix[4]arene (0.037 mmol) and dicyclohexylcarbodiimide (0.16 mmol) in dichloromethane (3 mL) was stirred for 10 min, and *para*-MAP (0.075 mmol) in dichloromethane (1 mL) was added and the mixture was stirred overnight. The solvent was removed, and the residue was dissolved in chloroform (50 mL) and washed with water (30 mL). The product was purified by flash column chromatography on silica gel. Where necessary, the silica gel was washed with 4 column volumes of hexane to remove dicyclohexylurea prior to elution of the amide.

5,11,17,23-Tetra-*tert*-butyl-25,27-di[methoxy(4-amidophenyl)-10,-15,20-tris-(*p*-methylphenyl)porphyrin]-26$-$28-dihydroxycalix[4]-arene, 2. A solution of 11,17,23-tetra-*tert*-butyl-25,27-dicarboxymethoxy-26,28-dihydroxycalix[4]arene (29.8 mg, 0.039 mmol) and dicyclohexyl-carbodiimide (33 mg, 0.16 mmol) was stirred for 10 min in dichloromethane (3 mL). 5-(*para*-Aminophenyl)-10,15,20-tris-(*para*-methylphenyl)porphyrin (50 mg, 0.075 mmol) in dichloromethane (1 mL) was added. Flash column chromatography with dichloromethane:hexane (1:1) gave **2** (43 mg, 54%). FAB-MS: found (M)$^+$ 2072 *m/z* for C$_{142}$H$_{130}$N$_{10}$O$_6$. ^{1}H NMR (C$_7$D$_8$): δ = -2.13 (s, 4 H, $-$N*H*$-$), 0.52 (s, 18 H, C(CH$_3$)$_3$), 1.17 (s, 18 H, C(CH$_3$)$_3$), 2.10 (s, 12 H, Ar$-$CH$_3$), 2.13 (s, 6 H, Ar$-$CH$_3$), 3.20 (d, *J* = 13.3 Hz, 4 H, Ar$-$CH$_2-$Ar), 4.19 (d, *J* = 13.3 Hz, 4 H, Ar$-$CH$_2-$Ar), 4.35 (s, 4 H, $-$OCH$_2$), 7.21 (d, *J* = 7.7 Hz, 8 H, Ar$-$CH$_2-$Ar), 7.25 (d, *J* = 7.9 Hz, 4 H, ArH), 7.27 (s, 8 H, ArH), 8.00 (d, *J* = 8.0 Hz, 12 H, ArH), 8.25 (d, *J* = 8.6 Hz, 4 H, ArH), 8.59 (d, *J* = 8.6 Hz, 4 H, ArH), 8.91 (s, 8 H, H$_\beta$), 9.11 (d, *J* = 4.8 Hz, 4 H, H$_\beta$), 9.31 (s, 2 H, CONH), 9.49 (d, *J* = 4.7 Hz, 4 H, H$_\beta$), 11.22 (s, 2 H, Ar$-$OH) ppm. UV$-$vis (toluene) λ_{max} (nm): ϵ (mol^{-1} L cm^{-1}), 421 nm (ϵ 449 657), 517 (ϵ 25 174), 551 (ϵ 16 527), 592 (ϵ 9633), 650 (ϵ 8090).

5,11,17,23-Tetra-*tert*-butyl-25,27-di[propoxy(4-amidophenyl)-10,-15,20-tris-(*p*-methylphenyl)porphyrin]-26$-$28-dihydroxycalix[4]-arene, 3. A solution of 5,11,17,23-tetra-*tert*-butyl-25,27-dicarboxypropoxy-26$-$28-dihydroxycalix[4]arene (31.5 mg, 0.037 mmol) and dicyclohexylcarbodiimide (33 mg, 0.16 mmol) was stirred for 10 min in dichloromethane (5 mL). 5-(*para*-Aminophenyl)-10,15,20-tris-(*para*-methylphenyl)porphyrin (50 mg, 0.075 mmol) in dichloromethane (2 mL) was added. Flash column chromatography with dichloromethane:hexane (1:1) gave **3** (42 mg, 54%). FAB-MS: found (M)$^+$ 2128 *m/z* for C$_{146}$H$_{138}$N$_{10}$O$_6$. ^{1}H NMR (CDCl$_3$): δ = -2.81 (s, 4 H, $-$N*H*$-$), 1.22 (s, 18 H, $-$C(CH$_3$)$_3$), 1.25 (s, 18 H, $-$C(CH$_3$)$_3$), 2.59 (s, 6 H, $-$CH$_3$), 2.70 (s, 12 H, $-$CH$_3$), 3.31 (t, *J* = 6.4 Hz, 4 H, CH$_2$), 3.31 (d, *J* = 12.9 Hz, 4 H, Ar$-$CH$_2-$Ar), 4.27$-$4.31 (m, 8 H, CH$_2$), 4.75 (d, *J* = 13.0 Hz, 4 H, Ar$-$CH$_2-$Ar), 6.99 (s, 4 H, ArH), 7.38 (d, *J* = 7.8 Hz, 4 H, ArH), 7.53$-$7.56 (m, 8 H, ArH), 7.94 (d, *J* = 7.8 Hz, 4 H, ArH), 8.07$-$8.10 (m, 8 H, ArH), 8.48 (s, 2 H, CONH), 8.74 (d, *J* = 4.7 Hz, 4 H, H$_\beta$), 8.79$-$8.85 (m, 12 H, H$_\beta$), 9.78 (s, 2 H, ArOH) ppm. UV$-$vis (toluene), λ_{max} (nm), ϵ (mol^{-1} L cm^{-1}): 421 nm (ϵ 413 334), 517 (ϵ 19 382), 552 (ϵ 11 841), 592 (ϵ 6276), 650 (ϵ 5537).

5,11,17,23-Tetra-*t*-butyl-25,27-di[methoxy(4-amidophenyl)-10,15,-20-tris(pentafluorophenyl)porphyrin]-26$-$28-dihydroxycalix[4]-arene, 4. A solution of 11,17,23-tetra-*tert*-butyl-25,27-dicarboxymethoxy-26,28-dihydroxycalix[4]arene (46 mg, 0.060 mmol) and dicyclohexyl-carbodiimide (51 mg, 0.25 mmol) was stirred for 10 min in dichloromethane (8 mL). 5-(*para*-Aminophenyl)-10,15,20-tris(C$_6$F$_5$)porphyrin (121 mg, 0.13 mmol) in dichloromethane (3 mL) was added. Purification using flash column chromatography with dichloromethane as eluent gave **4** (96 mg, 63%). FAB-MS: found (M)$^+$ 2528 *m/z* for C$_{136}$H$_{88}$-F$_{30}$N$_{10}$O$_6$. ^{1}H NMR (CDCl$_3$): δ = -2.90 (s, 4 H, $-$N*H*$-$), 1.19 (s, 18 H, $-$C(CH$_3$)$_3$), 1.32 (s, 18 H, C(CH$_3$)$_3$), 3.72 (d, *J* = 13.3 Hz, 4 H, Ar$-$CH$_2-$Ar), 4.49 (d, *J* = 13.3 Hz, 4 H, Ar$-$CH$_2-$Ar), 4.98 (s, 4 H, O$-$CH$_2$), 7.17 (s, 4 H, ArH), 7.24 (s, 4 H, ArH), 8.25 (d, *J* = 8.6 Hz, 4 H, ArH), 8.32 (d, *J* = 8.6 Hz, 4 H, ArH), 8.81$-$8.85 (m, 12 H, H$_\beta$), 9.30 (d, *J* = 4.7 Hz, 4 H, H$_\beta$), 11.20 (s, 2 H, OH) ppm. UV$-$vis (toluene) λ_{max} (nm), ϵ (mol^{-1} L cm^{-1}): 419 nm (ϵ 487 145), 511 (ϵ 38 547), 544 (ϵ 11 806), 588 (ϵ 13 010), 642 (ϵ 2879).

5,11,17,23-Tetra-*t*-butyl-25,27-di[methoxy(4-amidophenyl)-10,15,-20-tris-(3,5-di-*tert*-butylphenyl)porphyrin]-26$-$28-dihydroxycalix-[4]arene, 5. A solution of 11,17,23-tetra-*tert*-butyl-25,27-dicar-boxymethoxy-26,28-dihydroxycalix[4]arene (86 mg, 0.11 mmol) and dicyclohexylcarbodiimide (96 mg, 0.46 mmol) in dichloromethane (10 mL) was stirred for 10 min. 5-(*para*-Aminophenyl)-10,15,20-tris-(3,5-di-*tert*-butylphenyl)porphyrin (240 mg, 0.25 mmol) in dichloromethane (5 mL) was added. The mixture was stirred overnight, and **5** was then purified via flash chromatography using chloroform:hexane (1:2) as eluent (170 mg, 57%). FAB-MS: found (M + H)$^+$ 2663 *m/z* for C$_{184}$H$_{214}$N$_{10}$O$_6$ + H. ^{1}H NMR (CDCl$_3$): δ = -2.75 (s, 4 H, $-$N*H*$-$), 1.17 (s, 18 H, $-$C(CH$_3$)$_3$), 1.31 (s, 18 H, $-$C(CH$_3$)$_3$), 1.41 (s, 72 H, 10,20-C(CH$_3$)$_3$), 1.479 (s, 36 H, 15-C(CH$_3$)$_3$), 3.67 (d, *J* = 13.5 Hz, 4 H, Ar$-$CH$_2-$Ar), 4.48 (d, *J* = 13.6 Hz, 4 H, Ar$-$CH$_2-$Ar), 4.92 (s, 4 H, O$-$CH$_2$), 7.14 (s, 4 H, ArH), 7.21 (s, 4 H, ArH), 7.69 (t, *J* = 1.7 Hz, 4 H, ArH), 7.74 (t, *J* = 1.8 Hz, 2 H, ArH), 8.00 (d, *J* = 1.8 Hz, 8 H, ArH), 8.05 (d, *J* = 1.7 Hz, 2 H, ArH), 8.28 (s, 8 H, H$_\beta$), 8.85 (s, 2 H, NHCO), 8.81 (d, *J* = 5 Hz, 4 H, ArH), 8.83 (d, *J* = 5 Hz, 4 H, ArH), 8.99 (d, *J* = 4.6 Hz, 4 H, H$_\beta$), 9.14 (d, *J* = 4.1 Hz, 4 H, H$_\beta$), 11.10 (s, 2 H, OH) ppm. UV$-$vis (toluene) λ_{max} (nm), ϵ (mol^{-1} L cm^{-1}): 419 nm (ϵ 487 145), 511 (ϵ 38 547), 544 (ϵ 11 806), 588 (ϵ 13 010), 642 (ϵ 2879).

Zn$_2$5. A saturated solution of Zn(II) acetate in methanol (0.5 mL) was added to a solution of **5** (50 mg, 0.019 mmol) in chloroform (20 mL), and the mixture was refluxed until no free-base porphyrin was observed in the UV$-$vis spectrum. The solvents were removed, and **Zn$_2$5** was purified by flash chromatography using dichloromethane/ether (9:1) as eluent (38 mg, 73%). FAB-MS: found (M)$^+$ 2788 *m/z* for C$_{184}$H$_{210}$N$_{10}$O$_6$Zn$_2$. ^{1}H NMR (CDCl$_3$): δ = 1.18 (s, 18 H, $-$C(CH$_3$)$_3$), 1.32 (s, 18 H, $-$C(CH$_3$)$_3$), 1.42 (s, 72 H, 10,20-C(CH$_3$)$_3$), 1.49 (s, 36 H, 15-C(CH$_3$)$_3$), 3.68 (d, *J* = 13.4 Hz, 4 H, Ar$-$CH$_2-$Ar), 4.49 (d, *J* = 13.3 Hz, 4 H, Ar$-$CH$_2-$Ar), 4.93 (s, 4 H, O$-$CH$_2$), 7.15 (s, 4 H, ArH), 7.225 (s, 4 H, ArH), 7.70 (t, *J* = 1.5 Hz, 4 H, ArH), 7.75 (t, *J* = 1.6 Hz, 2 H, ArH), 8.02 (d, *J* = 1.6 Hz, 8 H, ArH), 8.05 (d, *J* = 1.7 Hz, 4 H, ArH), 8.31 (s, 8 H, ArH), 8.87 (s, 2 H, NHCO), 8.92 (d, *J* = 4.7 Hz, 4 H, H$_\beta$), 8.95 (d, *J* = 4.7 Hz, 4 H, H$_\beta$), 9.02 (d, *J* = 4.7 Hz, 4 H, H$_\beta$), 9.27 (d, *J* = 4.7 Hz, 4 H, H$_\beta$), 11.10 (s, 2 H, OH) ppm. UV$-$vis (toluene) λ_{max} (nm), ϵ (mol^{-1} L cm^{-1}): 423 nm (ϵ 695 333), 551 (ϵ 38 450), 590 (ϵ 11 371).

Cu$_2$5. A saturated solution of Cu(II) acetate in methanol (0.5 mL) was added to a solution of **5** (51 mg, 0.019 mmol) in chloroform (20 mL), and the mixture was refluxed until no free-base porphyrin was observed in the UV$-$vis spectrum. The solvents were removed, and **Cu$_2$5** was purified by flash chromatography using dichloromethane/ether (9:1) as eluent (43 mg, 81%). FAB-MS: found (M)$^+$ 2785 *m/z* for C$_{184}$H$_{210}$N$_{10}$O$_6$Cu$_2$. ^{1}H NMR (CDCl$_3$): δ = 1.16 (s, 18 H, $-$C(CH$_3$)$_3$), 1.28 (s, 18 H, $-$C(CH$_3$)$_3$), 1.39 (br s, C(CH$_3$)$_3$), 3.61 (br s, 4 H, Ar$-$CH$_2-$Ar), 4.36 (br s, 4 H, Ar$-$CH$_2-$Ar), 4.77 (br s, 4 H, O$-$CH$_2$), 7.11 (s, 4 H, ArH), 7.17 (s, 4 H, ArH), 7.60 (br s, ArH), 8.78 (br s, ArH), 10.89 (br s, H$_\beta$). UV$-$vis (toluene) λ_{max} (nm), ϵ (mol^{-1} L cm^{-1}): 417 nm (ϵ 666 274), 540 (ϵ 35 379).

Ni$_2$5. A saturated solution of Ni(II) acetate in methanol (0.5 mL) was added to a solution of **5** (48 mg, 0.018 mmol) in chloroform (20 mL), and the mixture was refluxed until no free-base porphyrin was observed in the UV−vis spectrum. The solvents were removed, and **Ni$_2$5** was purified via chromatography using dichloromethane ether (9:1) as eluent (44 mg, 89%). FAB-MS: found (M − 2H)$^+$ 2773 *m/z* for (C$_{136}$H$_{84}$F$_{30}$N$_{10}$O$_6$Ni$_2$ − 2H). ^{1}H NMR (CDCl$_3$): δ = 1.15 (s, 18 H, −C(CH$_3$)$_3$), 1.30 (s, 18 H, −C(CH$_3$)$_3$), 1.37 (s, 72 H, C(CH$_3$)$_3$), 1.43 (s, 36 H, C(CH$_3$)$_3$), 3.64 (d, *J* = 13.4 Hz, 4 H, Ar−CH$_2$−Ar), 4.43 (d, *J* = 13.2 Hz, 4 H, Ar−CH$_2$−Ar), 4.86 (s, 4 H, O−CH$_2$), 7.11 (s, 4 H, ArH), 7.19 (s, 4 H, ArH), 7.62 (t, *J* = 1.5 Hz, 4 H, ArH), 7.67 (t, *J* = 1.7 Hz, 2 H, ArH), 7.79 (d, *J* = 1.6 Hz, 8 H, ArH), 7.83 (d, *J* = 1.7 Hz, 4 H, ArH), 8.01 (d, *J* = 8.5 Hz, 4 H, ArH), 8.12 (d, *J* = 8.5 Hz, 4 H, ArH), 8.73 (s, 10 H), 8.77 (d, *J* = 5 Hz, 4 H, H$_\beta$), 8.97 (d, *J* = 5 Hz, 4 H, H$_\beta$), 10.94 (s, 2 H, OH) ppm. UV−vis (toluene) λ_{max} (nm), ϵ (mol^{-1} L cm^{-1}): 417 nm (ϵ 666 274), 540 (ϵ 35 379).

5,11,17,23-Tetra-*tert*-butyl-25,27-di[methoxy(4-amidophenyl)-10,-15,20-tris-(3,4,5-trimethoxyphenyl)porphyrin]-26−28-dihydroxycalix-[4]arene, 6. A solution of 11,17,23-tetra-*tert*-butyl-25,27-dicarboxymethoxy-26,28-dihydroxycalix[4]arene (20.4 mg, 0.014 mmol) and dicyclohexylcarbodiimide (21 mg, 0.10 mmol) in dichloromethane (5 mL) was stirred for 10 min. 5-(*para*-Aminophenyl)-[2,8,12,18-tetrabutyl-3,7,13,17-tetramethyl-15-(3,5-di-*tert*-butylphenyl)]-21*H*,23*H*-porphyrin (51 mg, 0.059 mmol) in dichloromethane (2 mL) was added, and the mixture was stirred overnight. The solvent was then removed, and the residues were dissolved in chloroform (50 mL) and washed with water (30 mL). Removal of solvent and flash chromatography with CHCl$_3$/heptane (1:1) gave porphyrin **6** (21 mg, 27%). FAB-MS:

found (M + H)$^+$ 2470 *m/z*. ^{1}H NMR (CDCl$_3$): δ = −2.37 (s, 4 H, −NH−), 0.95 (t, *J* = 7.4 Hz, 12 H, CH$_3$), 1.06 (t, *J* = 7.4 Hz, 12 H, CH$_3$), 1.15 (s, 18 H, −C(CH$_3$)$_3$), 1.35 (s, 18 H, −C(CH$_3$)$_3$), 1.49 (s, 36 H, C(CH$_3$)$_3$), 1.65 (q, *J* = 7.4 Hz, 8 H, C*H$_2$*CH$_3$), 1.71 (q, *J* = 7.4 Hz, 8 H, C*H$_2$*CH$_3$), 2.13 (m, *J* = 7.5 Hz, 8 H, C*H$_2$*CH$_2$CH$_3$), 2.45 (s, 6 H, CH$_3$), 2.61 (s, 6 H, CH$_3$), 3.69 (d, *J* = 13.4 Hz, 4 H, Ar−CH$_2$−Ar), 3.93−3.98 (m, 8 H, −C*H$_2$*CH$_2$CH$_2$CH$_3$), 4.50 (d, *J* = 13.3 Hz, 4 H, Ar−CH$_2$−Ar), 4.96 (s, 4 H, Ar−O−CH$_2$), 7.12 (s, 4 H, ArH), 7.78 (t, *J* = 1.7 Hz, 2 H, ArH), 7.90 (d, *J* = 1.75 Hz, 4 H, ArH), 8.17 (d, *J* = 8.5 Hz, 4 H, ArH), 8.34 (d, *J* = 8.5 Hz, 4 H, ArH), 8.53 (s, 2 H, NHCO), 10.20 (s, 4 H, *meso*-CH), 11.03 (s, 2 H, OH) ppm. UV−vis (toluene) λ_{max} (nm), ϵ (mol^{-1} L cm^{-1}): 412 nm (ϵ 385 051), 507 (ϵ 34 381), 539 (ϵ 9948), 576 (ϵ 13 715), 628 (ϵ 3386).

Supporting Information Available: Details of the synthesis and characterization of porphyrin and calix[4]arene precursors to compounds **1−6**. This material is available free of charge via the Internet at http://pubs.acs.org.

JA066031X